IEEE Robotics and Automation Letters (RAL) paper presented at the
2020 IEEE/RSJ International Conference on Intelligent Robots and Systems (IROS)
October 25-29, 2020, Las Vegas, NV, USA (Virtual)

Wide Area Exploration System Using Passive-Follower Robots Towed by Multiple Winches

Jose Victorio Salazar Luces, Manami Hoshi, and Yasuhisa Hirata

***Abstract*— In this study, we propose a wide area exploration system that consists on passive wheeled robots equipped with exploration sensors that are pulled from a high position with wires fed out from two winches. The robots are driven by the pulling force from the winches and they are able to steer by controlling brakes attached to their wheels. By adjusting the wire length, the passive-follower robot is pulled within the exploration area and it controls the braking torque of the wheels to follow a desired trajectory based on its current position. This system has the advantage that it is effective for ground exploration, does not require advanced calibration, and can be installed quickly. In this paper, we first explain the outline of the proposed system. Then, we introduce the hardware design of the developed winches and passive-follower robot. Next, the control method of the winch unit and the passive-follower robots are described. Here, we introduce the feasible braking control region for motion analysis and control of the passive-follower robot. Finally, we apply these control methods to the proposed system and report the results of verification experiments. We describe the feasible range of a follower robot, which changes depending on the position of the winches. We conducted an outdoor experiment, and confirmed the effectiveness of this system by evaluating the trajectories of the passive-follower robot.**

I. INTRODUCTION

Wide area exploration is necessary in multiple situations. For example, in recent years disasters such as earthquakes, landslides, and volcanic eruptions have frequently occurred in Japan, and exploration activities aimed at saving lives and collecting information have been of critical importance. As another example, ground exploration using magnetomectric instrumentation is useful for detecting possible mineral ores for mining, while ground penetrating radars can be used to detect buried utilities such as gas pipes or sewage in civil construction.

By using robots, exploration efficiency can be improved. For example, in [1], they use a drone to hang an electromagnetic sensor and find vehicles buried in a landslide disaster. There is also research on the use in volcanic areas. In [2], they introduced a scenario for robotic volcano observation, particularly the observation of ash in restricted areas. The idea is to transport a small ground robot using a multi-rotor UAV into the restricted area, and then navigate the robot downward along the volcano slope. As you can see from these examples, there are many scenes that require exploration near the surface. The problem of these studies are that the position and orientation of the sensor are likely to be unstable when the sensor is suspended by a drone, and that the wheel type mobile robot can get stuck depending on the ground conditions.

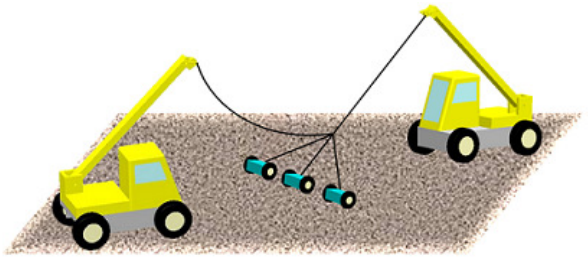

Fig. 1. Concept of Wide Area Exploration System

On the other hand, in order to realize a highly efficient system, research using multiple robots has been conducted [3]-[9]. For maintaining the formation of multiple robots, communication between robots [10], [11] and vision-based control methods [12], [13] have been proposed. However, the problem is that the system becomes complicated due to the increase in information to be communicated and processed. To solve this problem, Hirata et al. proposed a system consisting of an active leader and multiple passive-follower robots [14]. The followers are driven by being towed by the leader, and independently steer by controlling the difference in the rotation of the wheels using brakes [15] or an active braking force [16]. Formation control is possible as a whole by maintaining the relative position of each follower to the leader. In a verification experiment showing the effectiveness of this system, it was shown that formation can be controlled using a winch as a pseudo leader. In this verification experiment, the winch and the follower robot were installed in the same plane. Considering real life scenarios, there is a possibility that the surface obstacles and the tether interfere with each other and the formation control cannot be performed.

This problem can be solved by pulling the follower from a higher position, which can be done using winches. Wire-driven systems are suitable for observing predetermined points within a certain range because they can accurately control the position of the end-point [17]. In a previous study [18], a wire-driven system was successfully used for terrestrial ecosystem research with an investigation of the thermal properties of alpine plants. However, it is not suitable for exploration that requires ground contact, and it requires high-precision calibration to accurately control the position of the end-point.

*This work was partially supported by JAXA's Space Exploration Innovation Hub Center.

The authors are with Department of Robotics, Tohoku University, 6-6-01 Aramaki-Aoba, Aoba-ku, Sendai 980-8579, Japan. {j.salazar, m.hoshi, hirata}@srd.mech.tohoku.ac.jp

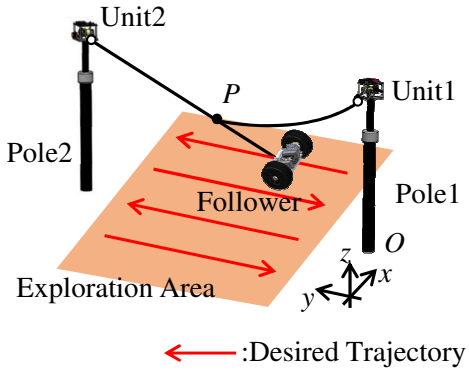

Fig. 2. Overview of the Principle Verification Model

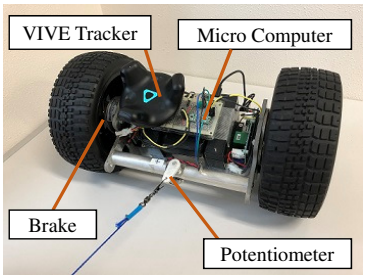

Fig. 3. Follower Robot

In order to solve these problems, this study proposes a system that combines multiple winches and passive-follower type robots as shown in Fig. 1. We call the passive-follower robot in this system the "follower". Winches are placed outside the exploration area, and the sensors necessary for exploration are mounted on the follower. The wire is fed out from the winch, and the follower is pulled from the connecting point. The follower is equipped with the positioning sensor like GPS, and its heading direction is controlled by brakes or steering motion to move to the desired position based on the measured position. This system has a similar configuration to Overburden Slushers [19] used in mining, which could be a potential use case of this system.

This system has four advantages: First, the follower can be pulled from a high position. This can prevent interference with surface obstacles. Also, as the torque to move the robot is provided by the cranes, it can climb slopes without requiring large motors on the robot. Second, it is useful for ground exploration. Since the sensor required for exploration is mounted on the follower, it is easy to stabilize the position and the orientation of the sensor. Furthermore, even if it gets stuck, the follower can be lifted temporarily by raising the position of the end-point using the wire and put down on the ground again. Third, it can be installed quickly and does not require highly accurate calibration as opposed to traditional wire-driven systems. The position of the end-point can be controlled approximately by the amount of wire fed, but when the follower steers, its position is passively shifted. However, precise position control is only required for the follower equipped with the sensor for the exploration, so it is acceptable that the position control of the end-point is not highly accurate. Due to this, it is possible to install it immediately in case of emergency such as landslide disaster. Fourth, it is a simple system. The control of the winch and the control of the follower are completely separate and do not require complicated communication. By using multiple followers, the efficiency can be expected to increase. In addition, since the follower is connected to the winch with a wire, there is a high possibility that the follower can be retrieved and data can be collected even if the system malfunctions.

The structure of this paper is as follows. First, an overview of the proposed system and the hardware configuration of the winch unit and the follower are introduced in section II. In section III, we describe the control of the winch unit. In section IV, we explain the steering control method of the follower using the feasible braking control region. In addition, we also describe the results of preliminary experiments on the transition limit of the follower. In section V, we conduct experiments using the system control methods described in section III and section IV, and confirm the effectiveness of this system. We report the results of the robot following a linear trajectory within the search area. Finally, section VI concludes this paper.

II. SYSTEM OVERVIEW AND HARDWARE CONFIGURATION

A. Wide Area Exploration System Using Multiple Winches and Passive-Follower Robots

In this subsection, we present an overview of the wide area exploration system using multiple winches and a passive-follower robot. To test the concept, we developed a principle verification model, shown in Fig. 2. We use a single follower and two winches attached to poles. We assign a number for each winch unit. The wires are fed from the winch units on the poles, and by adjusting the length of the wires, the position of the end-point can be changed. The tether from the follower is connected with the end-point. The follower acquires its own position information with a sensor such as GPS, and based on that information, follows the desired trajectory, represented as a red line in Fig. 2. In other words, the follower needs to accurately control its own position, but since it is obtained from the positioning sensor, the position information of the end-point is not required. Thus, it is not necessary to precisely control the position of the end-point. Also, since the follower uses a positioning sensor to estimate its own position in the global frame of reference, even if slip occurs, the robot can still pursue the target direction accordingly. As shown in the Fig. 2, by slacking the wire on the feeding side, the tension generated at the end-point is suppressed. In other words, the follower moves forward using the pulling force of the winch unit on the winding side. The follower controls the brakes attached on each wheel, resulting in a rotational difference in the wheels allowing it to steer. As the end-point goes back and forth changing the role of winding and feeding of winch units, the follower follows its motion within the exploration area. Also, the follower

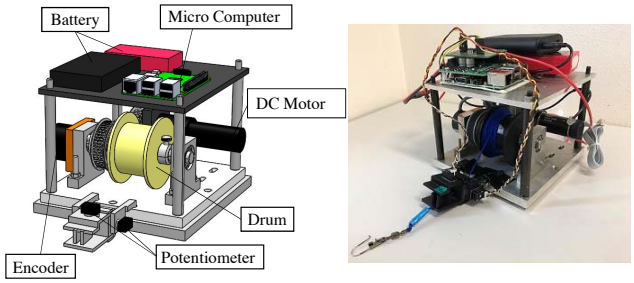

Fig. 4. Winch Unit

and the winch unit are controlled separately, and there is no communication between them.

B. Follower Hardware Configuration

The follower is shown in Fig. 3. The follower is an opposed two-wheel type robot with servo brakes attached to each wheel. The follower is equipped with a sensor for estimating its own position in the global frame of reference and a potentiometer for measuring the angle of the tether. The braking torque of each wheel is determined based on the information obtained from these sensors. We used a VIVE tracker as a sensor to estimate its own position for indoor experiments, which allows us to get the x, y coordinates of the follower on the ground within the exploration area. We selected powder brakes produced by Mitsubishi Electric. In the powder brake, the magnetic iron powder inside is magnetized by the exciting coil, and the iron powder is attracted to the wheel shaft and generates braking torque. Since torque is proportional to the excitation current over a wide range, the controllability is good. We use Raspberry Pi 3 Model B+ for controlling the follower. We use the position of the follower in the global frame of reference from the positioning sensor and the tether angle from the potentiometer as parameters for controlling the follower. We don't measure the tension force of the wire.

C. Winch Hardware Configuration

The winch unit is shown in Fig. 4. The unit has a two-stage configuration. The upper stage is equipped with a Microcomputer, a motor driver and batteries. The lower drive unit feeds and winds the wire by controlling the motor attached to the drum via the belt. To drive the winch unit, we selected a Maxon DC motor with an output of 20[W] and a rated voltage of 7.4[V]. The gear head has a gear ratio of 23: 1. The resolution of the encoder is 3600[P / R]. The diameter of the drum is 0.05[m]. By measuring the encoder value, it can be converted into the current wire feed amount. We use the encoder and potentiometer to measure the drum rotation and the angle of winding wire, and control the input voltage for the motor. We made two winch units with the same specifications.

D. Winch Unit Control Method

Fig. 5 shows a model of the system. In this figure, winch 1 is the feeding side and winch 2 is the winding side. Point O is the origin point which is the installation point of the pole of winch unit 1, point U_1 and U_2 are the position of the winch unit 1 and 2, point P is the end-point of wires, and point F is the position of the follower. We define y-axis is from Unit 1 to Unit 2, x-axis is vertical direction in the plane, and z-axis is vertical upward direction. Also, we define the parameters of the system as follows : $\overline{OU_1} = H$ (the height of the pole), $\overline{U_1U_2} = d$ (the distance between poles), W_{wind} and W_{feed} are the length of the winding and feeding side wire, W_F is the length of the tether from the end-point P to the follower, and β is the angle of the winding wire based y-z plane. β, W_{wind}, and W_{feed} can be measured with a potentiometer and an encoder on the winch unit, respectively.

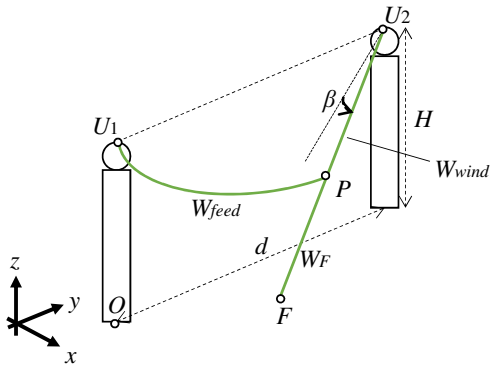

Fig. 5. System Modeling

The wire winding speed is made constant by controlling the rotational velocity of the motor. The velocity of the winding side unit determines the velocity of the follower. Since we mainly consider the robot's trajectory, strict velocity control of the follower is not necessary. The desired torque of the motor τ_d is determined by the following equation

$$\tau_d = k_v\{\omega_d(t) - \omega(t)\} + k_a \int \{\omega_d(t) - \omega(t)\}dt \qquad (1)$$

where $\omega_d(t)$ is the desired angular velocity of the motor, $\omega(t)$ is the current angular velocity of motor at time t and k_v, k_a are the controller's gain. The current rotational velocity $\omega(t)$ of the motor is measured using the measured value of the encoder. The input voltage V to the motor is determined by the following equation

$$V = R\frac{\tau_d}{k_i} + k_f\omega \qquad (2)$$

where R is internal resistance, k_f is the back-emf constant, and k_i is the torque constant.

The wire feeding speed is made constant, at the same rate as the winding side. As mentioned earlier, the system provides some slack on the wire on the feeding side to suppress the tension generated at the end-point P. Thanks to the slack, the setting of the two poles can be rough, calibration is not required, and the follower can be pulled by a single winch unit. In addition, the motion control can be reversed by swapping the role of the winch units. However, entanglement with surface obstacles due to excessive wire

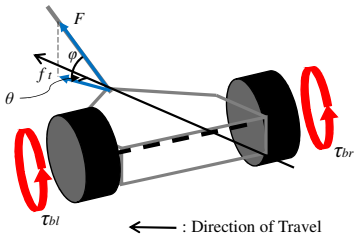

Fig. 6. Forces and Moments Acting on the Follower

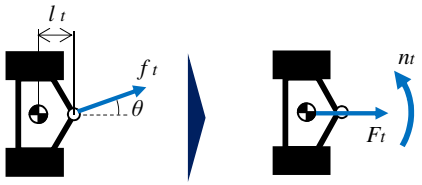

Fig. 7. Conversion Towing Force/Moment

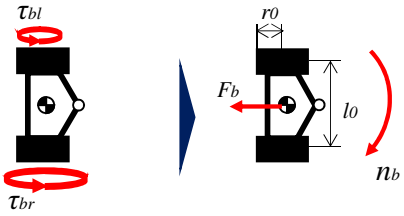

Fig. 8. Conversion Braking Force/Moment

slack must be avoided. Therefore, an algorithm for judging the slack and temporarily stopping the feeding of the wire when there is too much slack is required. We currently implemented an algorithm that uses geometric relationships, but this is not enough for judging the slack, and we think it will be necessary to develop a method using a tension sensor in the future.

III. MOTION CONTROL FOR THE FOLLOWER

A. Force and Moment Acting on the Follower

The follower is different from general active robots in that it is driven by an external force and controls their own braking torque. Therefore, we consider its motion from the forces and moments acting on the follower. Fig. 6 shows a model of the follower. In this figure, ϕ is the elevation angle of the tether with respect to moving plane, and θ is the angle in the moving plane. The wire pulling force F and the brake torque of each wheel act on the follower. We clarify this by converting the towing force acting on the follower and the brake torque generated on the wheels into the forces acting on the vehicle body and the moments around the center of gravity shown in Fig. 7, Fig. 8. In Fig. 7, $f_t = F\cos\phi$ is component of the tether's towing force in the moving plane, and l_t is distance from tether connection point to the follower's center of gravity. F_t is the force in the traveling direction of the towing force generated at the center of gravity, and n_t is the moment around the center of gravity,

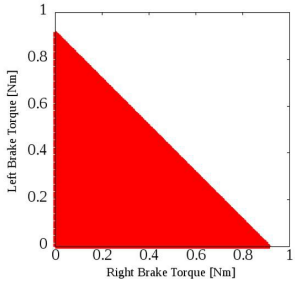

Fig. 9. Feasible Braking Torque

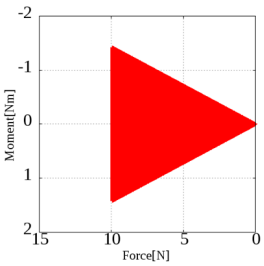

Fig. 10. Feasible Braking Control Region

and these are expressed as towing force/moment in the vector $X_t = [F_t\ n_t]^{\mathrm{T}}$. In Fig. 8, τ_{br} and τ_{bl} are the braking torque acting on right and left wheels respectively, r_0 is the wheel radius, and l_0 is the tread of the follower. F_b is the force in the braking direction of the braking force generated at the center of gravity, and n_b is the moment around the center of gravity, and these are expressed as the braking force/moment in the vector $X_b = [F_b\ n_b]^{\mathrm{T}}$. The towing force/moment $X_t = [F_t\ n_t]^{\mathrm{T}}$ and the braking force/moment $X_b = [F_b\ n_b]^{\mathrm{T}}$ can be expressed as follows:

$$X_t = \begin{bmatrix} F_t \\ n_t \end{bmatrix} = \begin{bmatrix} f_t\cos\theta \\ l_t f_t \sin\theta \end{bmatrix} \tag{3}$$

$$X_b = J^{\mathrm{T}^{-1}}\ \tau_b$$

$$J = \begin{pmatrix} \frac{r_0}{2} & \frac{r_0}{2} \\ \frac{r_0}{l_0} & -\frac{r_0}{l_0} \end{pmatrix} \tag{4}$$

B. Feasible Brake Force and Moment on the Follower

The braking torque generated on the follower wheels must satisfy the following conditions.

1. It must act in the opposite direction to the direction of wheel rotation.
2. It is within the range where the wheel does not slip.
3. It does not generate braking force higher than the traveling direction component of the towing force.

An example of a set of brake torques satisfying these conditions is shown in Fig. 9 (when $F = 15$[N], $\theta = 40$[deg], $\phi = 30$[deg]). In this figure, the horizontal axis represents the right brake torque, and the vertical axis represents the

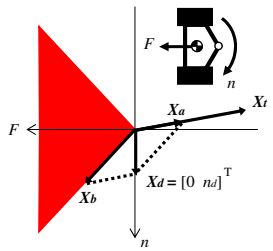

Fig. 11. Motion Control Based on Feasible Braking Control Region

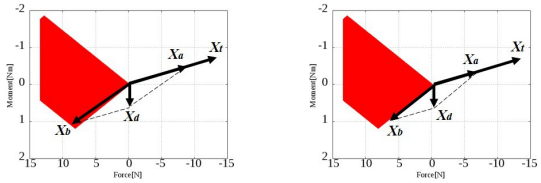

(a) Generating Braking Force/Moment in the Region (b) Generating Braking Force/Moment at the Border of the Region

Fig. 12. Feasible Braking Force/Moment

left brake torque. Using Eq.(4) on the set of feasible braking torques, we can derive the braking force/moment X_b that can be generated on the follower, depicted in Fig. 10[20].]. In this figure, the horizontal axis represents the braking force generated in the follower, and the vertical axis represents the brake moment generated around the center of gravity of the follower. This area is called the feasible braking control region. It is important to note that it doesn't represent a geometrical relationship. This is a useful concept for motion analysis and control of the follower. Its detailed derivation can be found in our previous work [15].

C. Motion Control Based on Feasible Braking Control Region

Since the motion of the follower is determined by the external pulling force/moment X_t and its own braking force/moment X_b, the motion control method becomes difficult compared to a robot with an active element such as a motor. In this subsection, we propose a follower motion control method based on the feasible braking control region.

We consider that follower moves on the line $x = x_{cur}$ and the desired line is $x = x_{des}$. Also, it is assumed that external pulling force/moment X_t is generated in the follower due to tether pulling. First, the moment n_d of force/moment $X_d = [F_d \ n_d]^{\mathrm{T}}$ on the follower required to move from the current position x_{cur} to desired position x_{des} at time t is given by the following equation.

$$n_d = K_p(x_{des} - x_{cur}) + K_i \int_0^t (x_{des} - x_{cur})dT - K_d \frac{dx_{cur}}{dt} \quad (5)$$

where K_p, K_i, and K_d represent the controller gains. Shown in Fig. 11, in order to generate the force/moment X_d necessary for steering, a part X_a of the external pulling force/moment X_t and the braking force/moment X_b in the feasible braking control region are used.

$$X_b = X_d - X_a \quad (6)$$

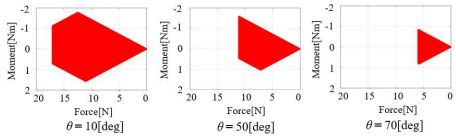

Fig. 13. Changes in Feasible Braking Control Region due to θ Changes ($F = 20$[N], $\phi = 30$[deg])

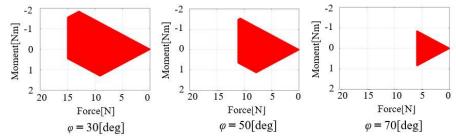

Fig. 14. Changes in Feasible Braking Control Region due to ϕ Changes ($F = 20$[N], $\theta = 30$[deg])

By determining the braking force/moment X_b so that X_t is as small as possible, the burden on the winch unit on the winding side can be reduced. As shown in Fig. 12, X_t becomes the smallest when the braking force/moment X_b is generated at the boundary of the region. By converting braking force X_b into braking torque τ_b using (7) and giving it to the wheels, the follower can steer according to the current position x_{cur} and the desired position x_{des}.

$$\tau_b = J^{\mathrm{T}} X_b \quad (7)$$

Fig. 13 and Fig. 14 show some examples of the change in shape of the feasible braking control regions based on the parameters. It can be seen that the larger the tether angle θ and the elevation angle ϕ, the smaller the feasible braking control region. As a result, the feasible braking force/moment X_b decreases, and there is a limit point where the required moment n_d cannot be generated. In this system, it is necessary to set the exploration area while considering this point. This is discussed in Section IV below.

IV. EXPERIMENT

A. Small Scale Experiment

We conducted experiments by applying the control methods described above to a wide area exploration system combining two winch units and the follower. The experimental setup is shown in Fig. 15. The winch unit is mounted on a tripod as shown in Fig. 15. The winch unit was set so that the pole height is H = 1[m], the distance between poles is d = 5[m], and the follower tether length is W_F = 0.5[m]. In this experiment, the winch unit controls the motor using the method proposed in section III. The desired feeding speed and winding speed were set to 0.2[m/s]. Based on the control method shown in section IV, the follower takes an initial position on $x = x_0$ and moves so as to transition to the desired positon $x = x_0 + 0.1$[m]. This experiment is carried out from x_0 = 0 to 0.4[m]. For comparison, we evaluated the change of the follower position from the initial position (x, y) = (0.3, 0.75), when the follower was not controlled.

Fig. 16 shows a comparison of the follower's paths with control and without control. When the follower was not

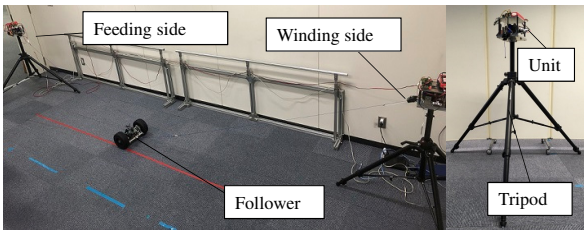

Fig. 15. Experimental Setup

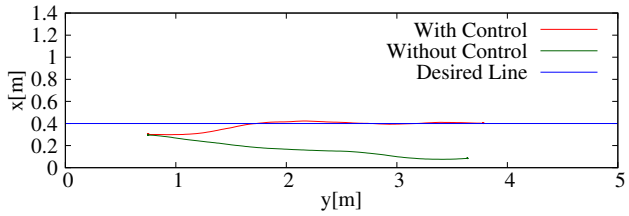

Fig. 16. Comparison of the Follower's Paths

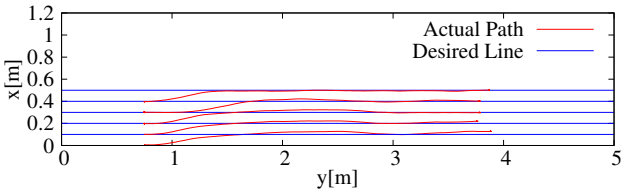

Fig. 17. Transition to Each Desired Straight Line

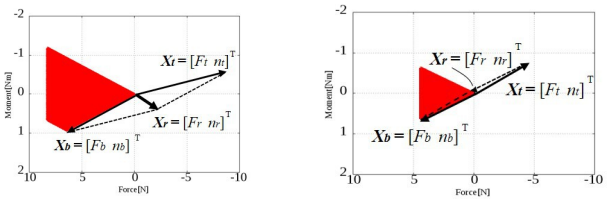

(a) Resultant Force/Moment X_r (b) Resultant Force/Moment X_r

Fig. 18. Transition Limit

controlled, it can be seen that the follower is pulled back to $x = 0$ by the pulling tension from the wire. On the other hand, the follower can successfully steer forwards the desired position when control is applied. Fig. 17 shows all follower's paths in this experiment. When the follower was controlled, we confirmed that it was able to reach each desired trajectory. From this experiment, the effectiveness of the proposed system and control method was confirmed.

For this paper, the experiments were performed with the follower moving in a single direction, but in the future we would like to enable the system to guide the follower towards the opposite direction automatically by either controlling the end-point and follower simultaneously to drive the follower in an U-turn motion or designing a follower that can be turned upside down and reverse the traveling direction.

B. Explorable Area

In this subsection, we derive the explorable area considering the motion characteristics of the follower. Motion of the follower is determined by the resultant force/moment $X_r = [F_r \ n_r]^{\mathrm{T}}$.The resultant force/moment $X_r = [F_r \ n_r]^{\mathrm{T}}$ is determined by the external pulling force/moment $X_t = [F_t \ n_t]^{\mathrm{T}}$ and its own braking force/moment $X_b = [F_b \ n_b]^{\mathrm{T}}$.

$$X_r = X_t + X_b \tag{8}$$

We show examples of the feasible braking control region and force/moment acting on the follower in Fig. 18. In Fig. 18(a) the resultant moment n_r can be generated in the opposite direction to the towing moment n_t, but in Fig. 18(b) the resultant moment n_r is in the same direction as the towing direction, and the follower is pulled back to the direction of the winding side winch unit. So, it is impossible to follow the desired straight line. Therefore, the condition for steering in the opposite direction to the towing by the wire is that the resultunt moment n_r determined by the towing moment n_t and the braking moment n_b is a positive value.

$$n_r = |n_b| - |n_t| > 0 \tag{9}$$

When the distance between the winch units $d = 18$[m], the height of the pole $H = 1.3$[m], and the desired straight line x_{des}=5.0[m], the change of the feasible braking control region is shown in Fig. 19. It can be seen that the closer to the winding side winch unit, the smaller the feasible braking control region and the smaller the moment n_r. In particular, when the y-coordinate value of the follower F_y is 15.9 [m], the resultant moment n_r is -0.10[Nm], and the follower cannot steer in the opposite direction to the towing moment n_t. It can be said that it can not follow the desired straight line and is pulled back toward the winch unit on the winding side. Given the height of the pole H and the distance between the winch units d, the range that satisfies the conditions in the exploration plane can be illustrated. This is defined as the explorable area. By considering this, we can determine the position of the winch units so that the area to be searched is included within the explorable area. It is important to mention that if the friction coefficient between the wheels and the ground becomes smaller on different grounds, the follower will easily slip. It means that the follower is more likely to be pulled back toward the winding side unit and the explorable area will become smaller.

C. Outdoor Experiment

We performed verification experiments using the developed prototype in an outdoor environment closer to a real situation. The experimental environment is shown in Fig. 20. The area to be searched is set to the 5[m]x10[m] rectangle, and we set desired straight trajectories for the follower starting at $x_0 = 0.0$[m], increasing in steps of 1.0[m] until $x = 5.0$[m] . In this experiment, as shown in Fig. 21, the robot transitions from the initial position x_0 to the desired line following the "transitiion" path, and then subsequently returns to the starting line y_0 via the "following" path. As a result, the follower can search the entire desired line while "following" the desired trajectory. The distance d between

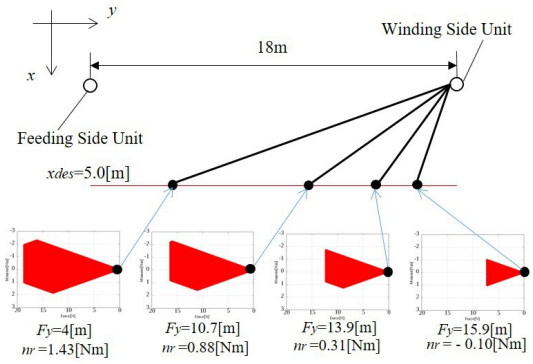

Fig. 19. Changes in Feasible Braking Control Region

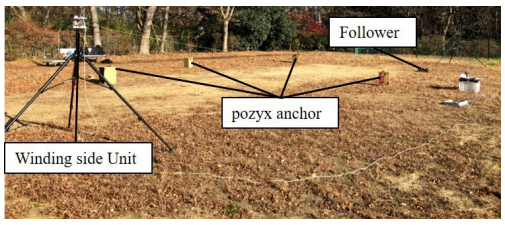

Fig. 20. Experiment in the Large Scale

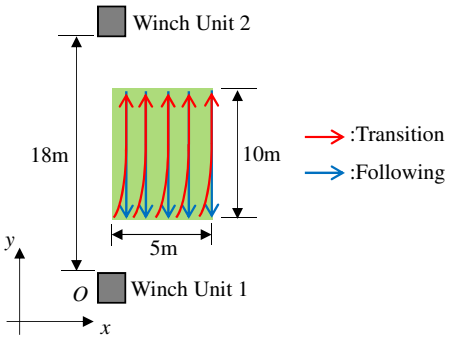

Fig. 21. Desired Trajectory

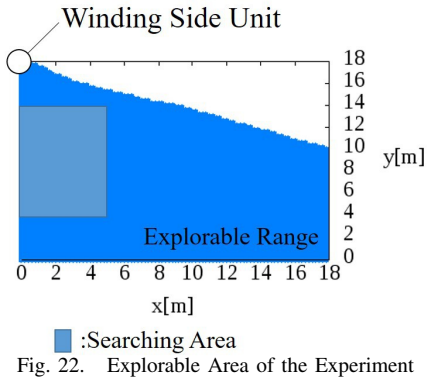

Fig. 22. Explorable Area of the Experiment

the towing units was set at 18[m], and the height H of the towing unit was set at 1.55[m]. At this time, it was confirmed that the target search range is covered with the explorable area shown in Fig. 22. Also, we used pozyx as a positioning sensor for the follower, given that its working principle is Ultra-Wide Band technology (UWB) and can be used outdoors. In addition, in this verification experiment, only the winding-side winch unit was used, under the assumption that the winch unit on the feeding side did not apply tension to the end-point P.

Fig. 23 shows the position data of pozyx used to control the follower. Fig. 23 (a) shows all trajectories of the follower. It can be seen that follower moves over the entire target search range. Fig. 23 (b)-(f) shows the trajectories of the follower following each desired straight line. It was confirmed that it was possible to follow all desired straight lines. As the desired straight line became larger, it was seen that the follower was pulled back to the winch unit on the winding side, but this is probably because the wire got tangled up in a part of the winch unit and generated more tension than expected. This will be improved in the future by installing a gimbal mechanism to enable smooth winding.

V. DISCUSSION

In this section we discuss the considerations needed to expand the verification model to the actual system based on the experimental results. In the verification experiment, we confirmed that even though the poles were roughly deployed, the follower could control the brake and follow the desired straight line using the proposed control method. It was also shown that by considering the explorable area, it is possible to decide the winch units position appropriately so that the robot can traverse the desired area entirely. As the feeding and winding are performed at constant speed, winches can be replaced by towing equipment such as large cranes. As a result, the towing power increases and we can increase the number of followers. In the future, it is necessary to further consider methods to maintain the slack on the feeding side wire.

The control method of the follower proposed this time is effective for following any path within the explorable area, and this control method can be applied to any two-wheeled robot that moves according to the difference in the amount of wheel rotation. For example, it may be possible to change to a robot with wheels equipped with lugs effective for running on rough terrain. In the future, the formation control will be performed as a whole by properly steering multiple followers, to explore a wider area simultaneously, thus increasing efficiency. However, increasing the number of tethers connected to the end-point P might cause it to swing. We need to consider the effect of this on the followers' motion.

VI. CONCLUSIONS

In this study, we proposed a wide area exploration system that combines multiple winches and a passive-follower robot. In the system, the winch units tow the follower equipped with sensors for exploration from a high position, while the follower robot controls its own position to follow a desired trajectory. This means that it's not necessary to control the end-point position of the winches accurately, so the system does not require any advanced calibration, and the winch units can be roughly placed in the environment. The feeding

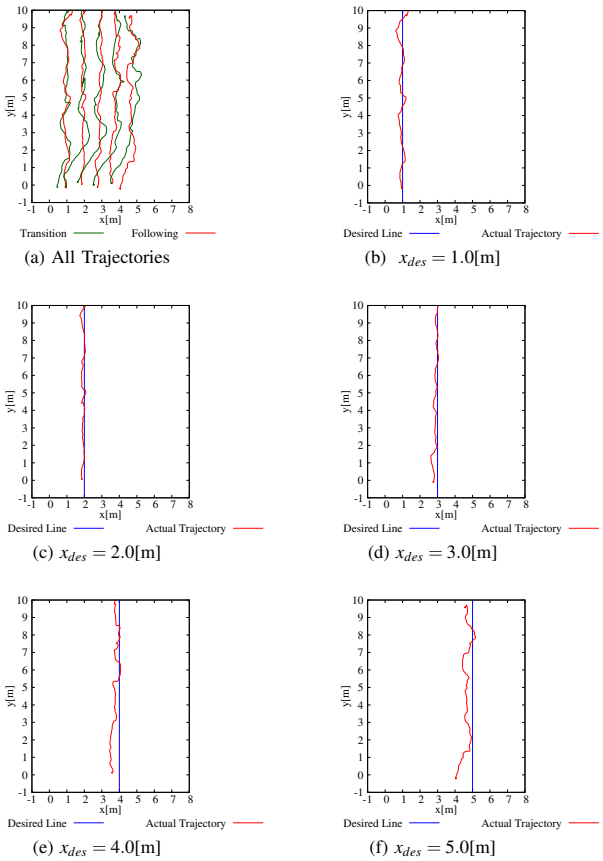

(a) All Trajectories (b) $x_{des} = 1.0$[m]

(c) $x_{des} = 2.0$[m] (d) $x_{des} = 3.0$[m]

(e) $x_{des} = 4.0$[m] (f) $x_{des} = 5.0$[m]

Fig. 23. Trajectories of the Follower

side winch unit provides some slack on the wire so that no force is applied to the end-point. As a result, the distance between winch units is not important as a control parameter, so the system can be installed quickly. The follower is driven by an external pulling force and steers by adjusting the braking torque of its own wheels. Using the concept of the feasible braking control region, we explained the motion control method and how to determine the explorable area. Next we conducted a verification experiment where the winch units pulled the follower, and the follower was able to reach the desired linear trajectories. In addition, we conducted an outdoor experiment considering the explorable area. Through these experiments, we demonstrated the feasibility of the proposed system and its control methods. Finally, we discussed about further considerations needed for developing a larger scale system with more followers.

In the future, we'd like to increase the number of the followers to two or more, in order to explore the area simultaneously, thus increasing the exploration efficiency. We would also like to study how the number of winch units affects the explorable area of the system, and how to determine the optimal number and position of winch units based on a desired explorable area.

REFERENCES

[1] "Aiming to Probe for Buried Vehicles Using a Drone After Landslides", https://www.aist.go.jp/aist-e/list/latest-research/2018/20180601/en20180601.html accessed on August 28, 2019.

[2] K. Nagatani et al., "Volcanic ash observation in active volcano areas using teleoperated mobile robots - Introduction to our robotic-volcano-observation project and field experiments," 2013 IEEE International Symposium on Safety, Security, and Rescue Robotics (SSRR), Linkoping, 2013, pp. 1-6, doi: 10.1109/SSRR.2013.6719324.

[3] J. Luo, C. Liu and F. Liu, "A leader-following formation control of multiple mobile robots with obstacle," 2015 IEEE International Conference on Information and Automation, Lijiang, 2015, pp. 2153-2158, doi: 10.1109/ICInfA.2015.7279644.

[4] T. Fong, C. Thorpe and C. Baur, "Multi-robot remote driving with collaborative control," in IEEE Transactions on Industrial Electronics, vol. 50, no. 4, pp. 699-704, Aug. 2003, doi: 10.1109/TIE.2003.814768.

[5] X. Yu and L. Liu, "Distributed Formation Control of Nonholonomic Vehicles Subject to Velocity Constraints," in IEEE Transactions on Industrial Electronics, vol. 63, no. 2, pp. 1289-1298, Feb. 2016, doi: 10.1109/TIE.2015.2504042.

[6] W. Ren, and N. Sorensen. "Distributed coordination architecture for multi-robot formation control," in Robotics and Autonomous Systems vol. 56, no. 4, pp. 324-333, 2008

[7] R. Wang, X. Dong, Q. Li and Z. Ren, "Distributed Adaptive Formation Control for Linear Swarm Systems With Time-Varying Formation and Switching Topologies," in IEEE Access, vol. 4, pp. 8995-9004, 2016, doi: 10.1109/ACCESS.2016.2646399.

[8] X. Dong, Y. Hua, Y. Zhou, Z. Ren and Y. Zhong, "Theory and Experiment on Formation-Containment Control of Multiple Multirotor Unmanned Aerial Vehicle Systems," in IEEE Transactions on Automation Science and Engineering, vol. 16, no. 1, pp. 229-240, Jan. 2019, doi: 10.1109/TASE.2018.2792327.

[9] X. Cai and M. d. Queiroz, "Adaptive Rigidity-Based Formation Control for Multirobotic Vehicles With Dynamics," in IEEE Transactions on Control Systems Technology, vol. 23, no. 1, pp. 389-396, Jan. 2015, doi: 10.1109/TCST.2014.2321664.

[10] R. Xue and G. Cai, "Formation Flight Control of Multi-UAV System with Communication Constraints," in Journal of Aerospace Technology and Management vol. 8, no. 2:203210, May. 2016.

[11] Y. Kantaros and M. M. Zavlanos, "Global Planning for Multi-Robot Communication Networks in Complex Environments," in IEEE Transactions on Robotics, vol. 32, no. 5, pp. 1045-1061, Oct. 2016, doi: 10.1109/TRO.2016.2593045.

[12] G. L. Mariottini et al., "Vision-Based Localization for Leader?Follower Formation Control," in IEEE Transactions on Robotics, vol. 25, no. 6, pp. 1431-1438, Dec. 2009, doi: 10.1109/TRO.2009.2032975.

[13] B. Fidan, V. Gazi, S. Zhai, N. Cen and E. Karata?, "Single-View Distance-Estimation-Based Formation Control of Robotic Swarms," in IEEE Transactions on Industrial Electronics, vol. 60, no. 12, pp. 5781-5791, Dec. 2013, doi: 10.1109/TIE.2012.2236996.

[14] H. Beglerovic, Y. Hirata and K. Kosuge, "Formation control of multiple passive type boats for sea surveillance," 2016 IEEE/SICE International Symposium on System Integration (SII), Sapporo, 2016, pp. 869-874, doi: 10.1109/SII.2016.7844109.

[15] Y. Hirata, K. Kimura, S. Matsuzaki, N. Ogawa and T. Kubota, "Control of Multiple Passive-Follower Type Robots Based on Feasible Braking Control Region Analysis," 2018 IEEE International Conference on Robotics and Automation (ICRA), Brisbane, QLD, 2018, pp. 5056-5061, doi: 10.1109/ICRA.2018.8460637.

[16] J. V. Salazar Luces, S. Matsuzaki and Y. Hirata, "RoVaLL: Design and Development of a Multi-Terrain Towed Robot with Variable Lug-Length Wheels," in IEEE Robotics and Automation Letters, doi: 10.1109/LRA.2020.3010495.

[17] P. H. Borgstrom et al., "Design and Implementation of NIMS3D, a 3-D Cabled Robot for Actuated Sensing Applications," in IEEE Transactions on Robotics, vol. 25, no. 2, pp. 325-339, April 2009.

[18] B. L. Jordan, M. A. Batalin and W. J. Kaiser, "NIMS RD: A Rapidly Deployable Cable Based Robot," Proceedings 2007 IEEE International Conference on Robotics and Automation, Roma, 2007, pp. 144-150.

[19] "Bosmin Overburden Slushers", available at https://bosmin.com//OS/osbrochure2.pdf accessed on June 17, 2020.

[20] Y. Hirata, Z. Wang, K. Fukaya and K. Kosuge."Transporting an Object by a Passive Mobile Robot with Servo Brakes in Cooperation with a Human", in Advanced Robotics, vol. 23, no. 4, 2009, pp. 387-404, doi: 10.1163/156855309X408745.